PCCP

ROYAL SOCIETY OF CHEMISTRY

PAPER

View Article Online
View Journal | View Issue

Cite this: *Phys. Chem. Chem. Phys.*, 2020, **22**, 11724

Influence of crowding on hydrophobic hydration-shell structure†

Aria J. Bredt and Dor Ben-Amotz *

The influence of molecular crowding on water structure, and the associated crossover behavior, is quantified using Raman multivariate curve resolution (Raman-MCR) hydration-shell vibrational spectroscopy of aqueous *tert*-butyl alcohol, 2-butyl alcohol and 2-butoxyethanol solutions of variable concentration and temperature. Changes in the hydration-shell OH stretch band shape and mean frequency are used to identify the temperature at which the hydration-shell crosses over from a more ordered to less ordered structure, relative to pure water. The influence of crowding on the crossover is found to depend on solute size and shape in a way that is correlated with the corresponding infinitely dilute hydration-shell structure (and the corresponding first hydration-shell spectra are invariably very similar to pure water). Analysis of the results using a Muller-like two-state equilibrium between more ordered and less ordered hydration-shell structures implies that crossover temperature changes are dictated primarily by enthalpic stabilization of the more ordered hydration-shell structures.

Received 7th February 2020,
Accepted 27th April 2020

DOI: 10.1039/d0cp00702a

rsc.li/pccp

Introduction

Crowding plays a central role in the self-assembly of biological, polymeric, and environmental systems.[1–4] Numerous prior theoretical[5–11] and experimental[12–23] studies have highlighted the influence of solute size[5–19] and crowding[20–23] on water structure and dynamics, as well as the associated water structural crossover,[5–18] but have not directly probed the influence of crowding on the crossover. Here we do so by measuring the hydration-shell vibrational spectra of aqueous solutions containing the three solutes shown in Fig. 1, using Raman multivariate curve resolution (Raman-MCR) spectroscopy.[24] Our results reveal that crowding decreases hydration-shell tetrahedrality and lowers the associated crossover temperature. However, we also find that the hydration-shells of these oily solutes are remarkably similar in structure to bulk water, even when the solution is sufficiently crowded that there is not enough water to fully populate the solute hydration-shell.

Early theoretical crossover predictions pertained to water containing idealized hydrophobic (hard-sphere) solutes,[5,6] and predicted a dramatic "dewetting" ("drying") crossover from a liquid-like to a vapor-like hydration-shell structure for hard-sphere solutes larger than ~1 nm, although subsequent theoretical studies predicted the suppression of both dewetting and solute aggregation by solute–water attractive interactions.[7,25,26] Experimental NMR,[12] single-molecule pulling,[13,14] Raman-MCR,[15–18] and THz[19] studies of aqueous solutions containing oily molecular and polymeric solutes confirmed the presence of a crossover length-scale near 1 nm at ambient temperatures, as well as a decrease in the crossover length-scale with increasing temperature (although the experimentally inferred changes in hydration-shell structure are less dramatic than a dewetting transition). The influence of crowding on water structure has previously been investigated using neutron-scattering measurements of concentrated alcohol–water mixtures.[20–23] The results, obtained with the aid of empirical potential structure refinement simulations, imply that water clusters non-randomly in highly crowded solutions, forming pools of nanometer size whose tetrahedral structure is similar to bulk water (while the alcohol molecules in these crowded solutions were found to cluster nearly randomly).[20] The present Raman-MCR results confirm the relative insensitivity of water structure to crowding,

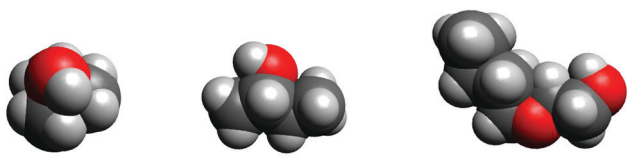

Fig. 1 Molecular structures of the three solutes.

Purdue University, Department of Chemistry, West Lafayette, IN 47907, USA. E-mail: bendor@purdue.edu

† Electronic supplementary information (ESI) available: Includes a description of the Muller-like two-state thermodynamic model, supplementary discussion of the relationship between hydration-shell spectral shape and crossover behavior, as well as additional experimental and MD results. See DOI: 10.1039/d0cp00702a

but also indicate that crowding tends to disrupt water structure, thus decreasing hydration-shell tetrahedrality and the associated crossover temperature.

Raman-MCR spectroscopy is uniquely suited to quantifying crossover phenomena, as the resulting spectra are exquisitely sensitive to small differences between the structure of pure water and the hydration-shell of a solute molecule. Prior Raman-MCR studies have quantified the influence of aggregation on hydration-shell structure,[18,24,27–29] but have not addressed the influence of crowding on hydrophobic crossover phenomena. The oily solutes shown in Fig. 1 were selected in part because of their relatively high aqueous solubility, which is required in order to establish the influence of crowding on hydration-shell structure. Note that a crowded solution is here defined as one in which there is not a sufficient amount of water to fully hydrate all the solute molecules. The results are analyzed using a Muller-like two-state model[30] and compared with previously published results to quantify the influence of solute size and shape on hydration-shell structure and crossover phenomena.

Results and discussion

The following is a detailed description of our experimental aqueous 2BA results, followed by a summary of the corresponding results for aqueous TBA and BE (with additional details provided in the ESI†). As will become evident, each of the three solutes are found to have different hydration-shell structures and crossover temperatures, both at infinite dilution and under crowded conditions, although the hydration-shell structures invariably remain quite similar to liquid water.

Fig. 2 compares the measured Raman spectra and Raman-MCR spectral components obtained from an aqueous 2BA solution of 0.5 M concentration at 20 °C. The dashed blue and dotted purple curves are the measured Raman spectra of pure water and aqueous 2BA. The solid purple curve is the Raman-MCR minimum area solute-correlated (SC) spectrum of 2BA, which contains features arising from the intramolecular vibrations of the solute (including the prominent CH stretch band near 2900 cm^{-1}) as well from hydration-shell water molecules that are perturbed by 2BA (as primarily evidenced in the OH stretch band between 3100 cm^{-1} and 3700 cm^{-1}). Note that previous studies have demonstrated that such SC OH bands arise primarily from perturbed water molecules, rather than the OH head group of the alcohol (due primarily to the far greater number of water OH groups in the hydration-shell).[15,31] The SC OH band highlights solute-induced perturbations in the OH stretch band of water, as more clearly seen in the inset panel in Fig. 2, which reveals that the SC OH spectrum also contains a small high frequency OH peak near 3660 cm^{-1} resulting from an increased population of non-hydrogen bonded (dangling) OH groups in the hydration-shell.[31,32] Moreover, the lower frequency hydrogen-bonded region of the SC OH stretch band has a different shape than the OH band of pure water, with a lower (red-shifted) average OH frequency and a more prominent shoulder near 3200 cm^{-1}, both of which imply

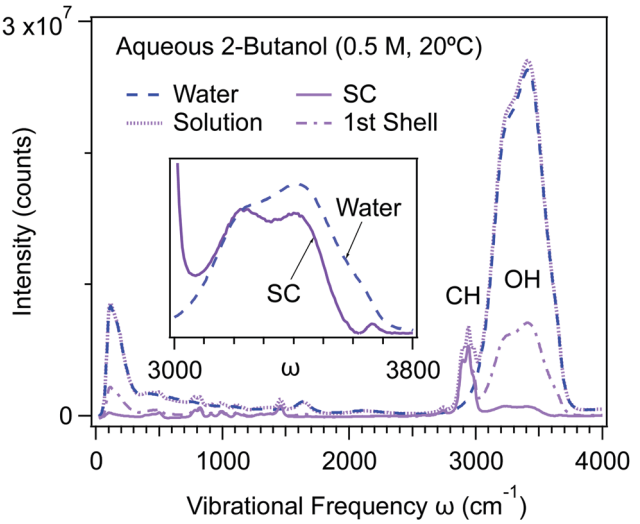

Fig. 2 Raman spectra of pure water (dashed blue curve) and a 0.5 M aqueous solution of 2BA (dotted purple curve) are compared with the resulting Raman-MCR SC (solid purple curve) and reconstructed first hydration-shell (dot-dash purple curve) spectra. The inset panel compares an expanded view of the OH stretch bands of pure water and the SC spectrum of 2BA (arbitrarily scaled to highlight the differences between the shapes of the pure water and SC OH stretch bands).

that the hydration-shell has a more tetrahedral structure than pure water at this temperature.[15,16]

The dot-dashed purple curve in Fig. 2 shows the reconstructed spectrum arising from the full first hydration-shell of 2BA. This first hydration-shell spectrum was obtained from a linear combination of pure water and SC spectra, constructed using an MD simulation-based estimate of the number of water molecules in the first hydration-shell (obtained as previously described, and further detailed in the ESI†).[16,17] More specifically, the MD results indicate that there are ~28 water molecules in the first hydration-shell of 2BA at 0.5 M and 20 °C (see ESI† Fig. S8 and Table S2). Since a 0.5 M aqueous solution contains a total of approximately 100 water molecules per solute, the MD results imply that nearly 1/3 of all the water molecules in the solution reside in the 2BA's first hydration-shell at this concentration. More specifically, the reconstructed first hydration-shell spectrum is obtained assuming that the average Raman cross section of water molecules in the first hydration-shell is the same as that in bulk water,[24] and the hydration-shell spectrum is reconstructed from a linear combination of the SC and pure water spectra so as to produce a hydration-shell spectrum whose OH band has an area consistent with first hydration-shell coordination number obtained from the MD simulations.

Fig. 3 shows how varying the temperature and concentration of the solution influence the SC and first hydration-shell spectra of 2BA. The temperature dependence of the SC spectra in solutions of 0.5 M and 2 M concentration are shown in Fig. 3(A) and (B), respectively, with expanded views in the inset panels. Note that all these SC spectra are normalized to the CH band area, and thus the decrease in the SC OH band area with increasing temperature implies that the hydration-shell

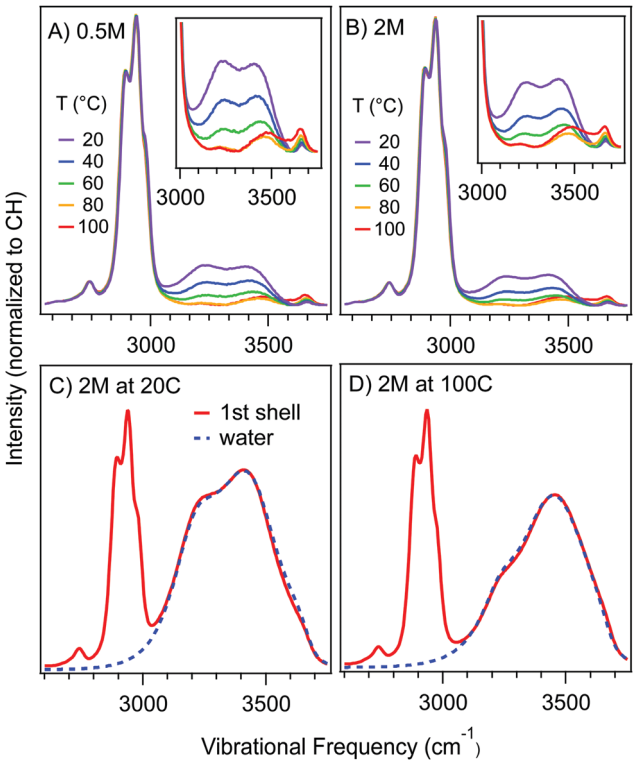

Fig. 3 The influence of temperature and concentration on the Raman-MCR SC spectra of aqueous 2BA, in the solute CH and hydration-shell OH band regions. (A) and (B) compare the temperature dependence of the SC spectra at solute concentrations of 0.5 M and 2 M. All the SC spectra are normalized to the CH band area, and thus represent the average SC spectra of a single solute. The inset panel of (A) and (B) contain an expanded view of the SC hydration-shell OH bands, all plotted with the same intensity scale. Panels (C) and (D) compare the OH stretch region of the full first hydration shell of 2 M 2BA (solid red) with bulk water (dashed blue) at 20 °C and 100 °C, scaled to the same OH band peak height in order to highlight the very similar, but slightly shifted, shapes of the hydration-shell and pure water OH bands.

structure differs most from pure water at low temperatures, and becomes most similar to pure water near 80 °C.

Comparison of the SC OH band areas shown panels Fig. 3(A) and (B) further indicates that at high concentration there are fewer perturbed water molecules in the hydration-shell of each solute – as evidenced, for example, by the difference between the areas of the 20 °C (purple) SC OH bands in (A) and (B). This decrease is consistent with the crowding-induced expulsion of water molecules from the solute's hydration-shell, as previously observed in other aqueous solutions.[27–29] Moreover, the change in shape of the SC OH band reveals that crowding leads to a decrease in the relative intensity of the hydration-shell 3200 cm^{-1} shoulder, which implies a decrease in water tetrahedrality.[15] It is also noteworthy that upon crowding the dangling OH peak frequency increases towards the ~3680 cm^{-1} frequency of dangling OH groups at a macroscopic air–water interface.[33] For example, at 20 °C the dangling OH frequency in the hydration-shell of TBA increases from ~3664 cm^{-1} at 1 M to ~3674 cm^{-1} at 4 M (corresponding to a solute volume fraction ~0.35), while that of BE increases from ~3668 cm^{-1} at 1 M to ~3676 cm^{-1} at 3 M (corresponding to a solute volume fraction ~0.36). This suggests that under crowded conditions, the water dangling OH groups exist in a lower local density environment than that in the hydration-shells of a dilute oily solutes.[34]

Fig. 3(C) and (D) compare the OH band of pure water with the full first hydration-shell spectrum of 2BA at a concentration of 2 M and either 20 °C (C) or 100 °C (D), obtained as described above (with further details in the Experimental and data analysis methods section, and the ESI†).[16,17] The striking similarity of the pure water (dashed blue) and first hydration-shell (solid red) OH bands implies that the structure of water in the first hydration-shell is extremely similar to that of pure water. However, close inspection of the hydration-shell and pure water OH bands reveals that at 20 °C the hydration-shell OH band is slightly red-shifted (lower in frequency) than pure water, while at 100 °C the hydration-shell is slightly blue-shifted (higher in frequency) than pure water. These very subtle frequency shifts can be quantified by obtaining the average OH frequency, as follows, where ω is the OH vibrational frequency the $I(\omega)$ is the OH band shape (normalized to unit area between ω_1 = 3200 cm^{-1} to ω_2 = 3800 cm^{-1}).

$$\langle\omega\rangle = \int_{\omega_1}^{\omega_2} \omega I(\omega) d\omega \quad (1)$$

The resulting average OH frequency shifts $\Delta\omega = \langle\omega\rangle - \langle\omega\rangle_0$, where $\langle\omega\rangle_0$ is the average OH frequency of pure water, are plotted in Fig. 4 as a function of both temperature and solute concentration.

The solid curves in Fig. 4 correspond to first hydration-shell frequency shifts, and the colors of the curves darken with increasing solute concentration (the significance of the dashed curves is further explained below). The inset panel shows an

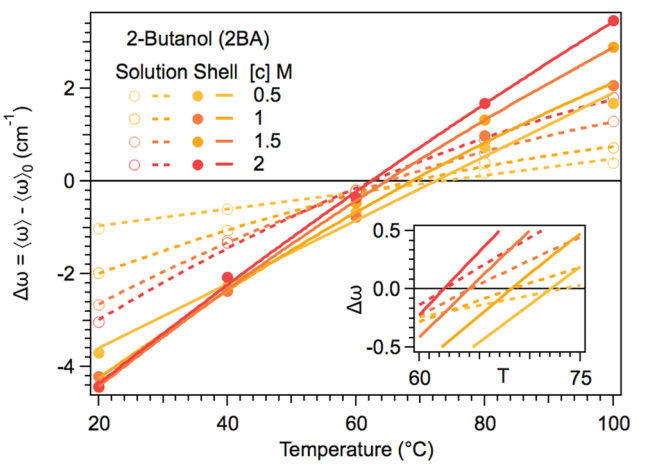

Fig. 4 Hydration-shell structural crossover is quantified by comparing the average OH frequency in the hydration-shell with that of pure water as a function of solute concentration. The crossover may be obtained either from the OH bands of the Raman-MCR reconstructed first hydration-shells (solid points and lines), or from the OH bands of the measured solution and water spectra (open points and dashed lines). Both procedures yield the same crossover temperatures that decrease with increasing solute concentration, as is more clearly evident in the inset panel showing an expanded view of the crossover region.

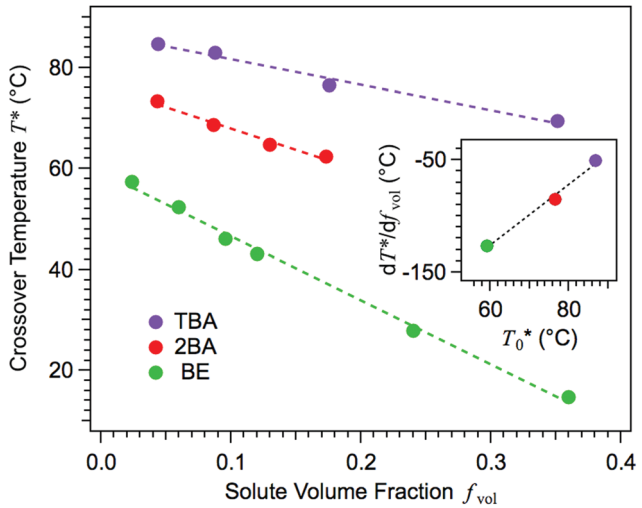

Fig. 5 The dependence of crossover temperature T^* on solute volume fraction. The y-intercept represents the crossover temperatures at infinite dilution T_0^*. The inset panel shows the correlation between T_0^* and the derivative of T^* with respect to solute volume fraction.

expanded view of the crossover region, thus more clearly revealing the temperatures at which the average OH frequency of the hydration-shell crosses over from negative (red-shift) to positive (blue-shift) values, relative to pure water. These zero-crossing temperatures are those at which the hydration-shell structure most closely resembles that of pure water, and the sign of $\Delta\omega$ (away from the zero-crossing point) indicates whether the hydration-shell is more ordered (negative) or disordered (positive) than pure water. These results reveal that, even over this relatively low concentration range, crowding decreases the crossover temperature by more than 10 °C, from a crossover temperature of ~72 °C at 0.5 M to ~62 °C at 2 M.

The results shown in Fig. 4 also demonstrate the insensitivity of the crossover temperatures to the assumed hydration-shell coordination number. This is most clearly illustrated by the dashed lines in Fig. 4, which represent the OH frequency shifts obtained directly from the measured solution and pure water OH bands. In other words, the dashed lines are obtained assuming that all the water molecules in the solution are in the hydration-shell of the solute. The crossover temperatures obtained from the dashed and solid lines are evidently essentially identical (as more clearly seen in the inset panel). However, the frequency shifts (away from the zero-crossing point) decrease with increasing hydration-shell size, as expected, since including more distant water molecules in the hydration-shell increases the spectral similarity of the hydration-shell and pure water. Further implications of the insensitivity of the crossover temperature to hydration-shell size are discussed in the Conclusions and implications section (as well as in Section 2 of the ESI†).

At a 2BA concentration of 2 M approximately 17% of the system volume is occupied by the solute. Note that the alcohol volume fraction, f_{vol}, is equivalent to the product of its concentration and its partial molar volume ($\bar{\nu}_{2BA} \approx 0.0866$ M^{-1}, so $f_{vol} = [c]\bar{\nu} = 2 \times 0.0866 \approx 0.173$).[35] Since this concentration is near the solubility limit of 2BA it is not possible to obtain crossover results at higher concentrations. However, the other two solutes, TBA and BE, are infinitely miscible in water (near ambient temperatures). Our crossover results obtained for those solutes extend up to solute volume fractions near 40% (obtained using $\bar{\nu}_{TBA} \approx 0.0878$ M^{-1} and $\bar{\nu}_{BE} \approx 0.12$ M^{-1}),[29,35] and have a correspondingly larger crowding-induced shift in the crossover temperature, as shown in Fig. 5. The hydration-shell OH band spectra of these more-crowded solutions still look strikingly similar to the OH bands of pure water (as shown in ESI† Fig. S4–S6, which also includes crossover results obtained assuming that the hydration-shell coordination number is concentration independent). Note that when fully hydrated the first hydration-shells of the three solutes in Fig. 1 contain approximately 30–40 water molecules (see ESI† Fig. S8). This implies that above a concentration of ~1 M, or a volume fraction of ~10%, there is no longer enough water to fully hydrate each solute, and thus such solutions are classified as crowded.

Fig. 5 shows a plot of the crossover temperature, T^*, as a function of volume fraction for the three solutes in Fig. 1. The crossover temperatures all decrease upon crowding, but each of the solutes has a different crossover temperature at infinite dilution T_0^* (as obtained from the y-intercepts of the dashed lines in Fig. 5) and a different slope with respect to volume fraction. The inset in Fig. 5 shows the correlation between the latter crowding-induced slope and the hydration-shell crossover at infinite dilution (along with the dotted best fit line $dT^*/df_{vol} = 2.74T_0^* - 290$). Thus, solutes with higher crossover temperatures at infinite dilution are also less sensitive to crowding. In other words, hydration-shells that are more ordered at infinite dilution are also less susceptible to crowding-induced disordering.

Conclusions and implications

Our results reveal that in both dilute and crowded solutions the hydration-shells of oily molecules are more ordered (more tetrahedral) than bulk water below the crossover temperature (T^*), and becomes more disordered above T^*. The associated changes in water tetrahedrality may be quantified by measuring the difference between the average OH frequency in bulk water and the hydration-shell. More specifically, previous experimental and MD simulation studies of pure water have revealed that there is a nearly linear correlation between the average OH frequency and tetrahedrality of water, such that $dq/d\omega \approx -0.00173$,[16] where q is the Errington–Debenedetti[36] tetrahedral order parameter. Thus, a red-shift of the average OH frequency of water corresponds to an increase in water tetrahedrality (or conversely for a blue-shift). Given that average tetrahedrality of water at 20 °C is $q \approx 0.67$, an OH frequency shift of $\Delta\omega = 4$ cm^{-1} (comparable to the largest shifts shown in Fig. 4) corresponds to a tetrahedrality change of ~1%, whose small magnitude is consistent with observed similarity of the pure water and hydration-shell OH bands, as shown in the Fig. 3(C) and (D). Note that the correlation between ω and q is only applicable to systems with hydration-shell OH stretch

band shapes that closely resemble bulk water, as is the case in the present studies. Moreover, the observed crossover behavior requires that the hydration-shell has a temperature dependent spectral shape, implying the presence of sub-populations of differing temperature dependence, as is evident in both Raman-MCR[15–17] and THz[19] hydration-shell spectra (and further discussed in the ESI†).

Previous studies have shown that the hydration-shell structural crossover in aqueous *n*-alcohol solutions is influenced by the length of the alcohol's oily tail, as well as by its OH head group, as the crossover temperature increases from ~60 °C for *n*-butanol to ~160 °C for methanol, but decreases to ~80 °C for methane.[16,17] This suggests that the crossover temperature is correlated with solutes size, and is increased by the presence of a polar head group. The previously measured crossover temperatures for short-chain *n*-alcohols (up to *n*-butanol) are approximately linearly correlated with solvent accessible surface area (SASA), such that T^* increases by 1 °C when SASA decreases by ~1 Å^2 (where SASA is obtained assuming a water radius of 1.4 Å). Moreover, comparison of T^* for the three butanol isomers, *n*-butanol, 2BA and TBA, with 1, 2, and 3 methyl groups, respectively, implies that T^* increases by ~6 °C for each solute methyl group. More specifically, a global correlation of the experimental crossover temperatures at infinite dilution for all of the above alcohol solutes (excluding BE) implies that $T_0{}^*$ (°C) = $314.9 - 1.026 \times \mathrm{SASA} + 6.36 \times n\mathrm{CH_3}$ (where $n\mathrm{CH_3}$ is the number of methyl groups per solute). This correlation reproduces the experimental crossover temperatures of all these alcohols to within a few degrees (as shown in the ESI† Table S1). However, this correlation does not hold for BE, as its crossover temperature is ~59 °C, which is similar to that of *n*-butanol although BE has a 33% larger SASA of ~336.8 Å^2 (and both solutes have the same number of methyl groups, $n\mathrm{CH_3} = 1$). Thus, the ether oxygen in BE evidently has the effect of increasing T^* by ~84 °C above that expected for an alcohol of approximately the same size and shape (*e.g.* *n*-heptanol). An alternative interpretation of the similar T^* values of BE and *n*-butanol is that T^* is dictated primarily by the *n*-butyl chains of these two solutes (and thus that the ethoxy ethyl head group of BE has approximately same influence on T^* as the OH head group of *n*-butanol).

The formation of perfectly tetrahedral clathrate hydrate solids containing methane and other small oily solutes,[37] implies that clathrate-like structures have a lower (more negative) enthalpy and entropy than liquid-like water structures. In other words, the transformation from a less ordered (liquid-like) to a more ordered (clathrate-like) structure at low temperatures indicates that clathrate formation is associated with a decrease in both enthalpy ($\Delta H < 0$) and entropy ($\Delta S < 0$). Although, the hydration-shells of oily molecules in liquid water are clearly not solid clathrates, the low temperature hydration-shell spectrum of methane dissolved in liquid water may be accurately represented as a linear combination of pure liquid water and clathrate structures.[17] Moreover, the hydration-shell of methane in liquid water qualitatively resembles the hydration-shells of 2BA, TBA, and BE, and all these oily molecules have hydration-shell structures that are very similar to liquid water.[16,17]

Additional physical insight regarding the influence of crowding on hydration-shell crossover behavior may be obtained by invoking a simple two-state model (in the spirit of the Muller model)[30] to describe the transformation of water from a less ordered to the more ordered structure (as further described in the ESI†). This analysis suggests that the observation of a crossover temperature requires that ΔH and ΔS in the hydration-shell of an oily solute (ΔH_S and ΔS_S) are not the same as in bulk water (ΔH_B and ΔS_B). Moreover, the observation of a crossover temperature implies that $\Delta H_S < \Delta H_B < 0$ and $\Delta S_S < \Delta S_B < 0$, and $T^* = (\Delta H_S - \Delta H_B)/(\Delta S_S - \Delta S_B)$ (as further explained in the ESI†). Additionally, this simplified two-state analysis suggests that an increase in T^* results from a greater enthalpic stabilization of the ordered (clathrate-like) water structure, relative to the disordered water structure. Furthermore, the observation that T^* decreases both with increasing solute size and crowding implies that the ordered water structure is enthalpically destabilized around large oily solutes and in crowded (oil-rich) solutions. This conclusion is consistent with the observation that increasing either solute size or crowding leads to a breakdown in water tetrahedrality. It is also consistent with the expectation that water near contacting (crowded) oily molecules is disrupted in a way that is qualitatively similar to water around a single larger oily molecule.

In summary, we have quantified the influence of crowding, as well as solute size and shape, on hydration-shell structure, and the associated crossover behavior. However, these results have not addressed the question as to how such water structure changes may influence the water-mediated interactions between oily molecules, including those leading to the self-assembly supramolecular structures such as micelles, vesicles, and bilayers. Theoretical and simulation studies by David Chandler and co-workers have suggested an intimate link between hydrophobic crossover (*i.e.* drying or dewetting) phenomena and the water-mediated aggregation/collapse of oily molecules.[7] However, it is not yet clear how to reconcile this view with the results of recent studies[25,26] (and prescient earlier work[38]) pointing to the importance of oil–water attractive (van der Waals) interactions in opposing the aggregation of oily molecules, given that such oil–water van der Waals interactions are expected to be relatively insensitive to water structure. Moreover, recent theoretical,[39] simulation,[40] and experimental[18] studies have reached conflicting conclusions regarding whether the collapse and clouding of oily polymers in water follows[39,40] or precedes[18] dehydration, thus raising further questions regarding the view that hydrophobic collapse is driven by dewetting-related crossover behavior.[39] Additionally, both recent and numerous prior studies[41] indicate that water penetrates deeply into micelles, thus suggesting that the high interfacial tension of macroscopic oil–water interfaces is greatly reduced at molecularly rough nonpolar interfaces of micelles composed of either cationic and anionic surfactants. Neutron scattering studies[20–23] have directly addressed the relationship between water structure, crowding, and aggregation in highly concentrated alcohol–water mixtures, and found that water tends to cluster non-randomly in pools of nanometer dimension and highly tetrahedral structure, while

the alcohol molecules in these solution are found to have a nearly random structure that is remarkably insensitive to water hydrogen-bonding and clustering.[20] Although these disparate findings remain to be fully reconciled with each other, the emerging picture suggests that the propensity of oily molecules to form crowded aggregates and collapsed structures in water is dictated substantially by competing oil–oil and oil–water van der Waals interactions, rather than by the relatively subtle changes in water structure associated with the crossover phenomena that we have experimentally observed using hydration-shell vibrational spectroscopy.

Experimental and data analysis methods

tert-Butyl alcohol (TBA), 2BA and 2-butoxyethanol (obtained from Sigma-Aldrich) were weighed and dissolved in water from a Millipore purification system (H_2O, 18.2 MΩ cm from Milli-Q UF plus) in 10 ml volumetric flasks. After mixing, each sample was pipetted into a 1 cm glass cuvette and capped. All samples were prepared and used within 24 h.

Raman spectra were obtained with a custom-built Raman system as previously described[42] using an Ar-ion excitation laser (514.5 nm, ~20 mW power at the sample), a 300 mm focal length spectrograph (SpectraPro300i, Acton Research Inc.), a grating of 300 grooves per mm and a TE cooled CCD camera (Princeton Instruments Inc. Pixis 400B). The samples were temperature controlled to a stability of better than ±0.1 °C over a temperature range of 20 °C to 100 °C using a TE cooled cell holder (Quantum Northwest).[43]

Raman-MCR spectra were obtained using self-modeling-curve-resolution (SMCR)[44] to decompose the measured solution spectra into pure solvent and minimum area solute-correlated (SC) components. The minimum area (non-negative) SC spectra were obtained relative to the local linear baseline of the SC spectra. First hydration-shell spectra were reconstructed from the pure water and background-subtracted SC spectra using hydration-shell coordination numbers (CN) obtained from MD simulation, as previously described (and further explained above and in the ESI†).[16,17]

The first hydration-shell spectrum was obtained by adding a scaled version of the pure water component to the SC spectrum such that the ratio of the resulting OH band area (integrated from 3200 cm^{-1} to 3800 cm^{-1}) divided by the CH band in the SC spectrum (integrated from 2795 cm^{-1} to 3045 cm^{-1}) is equal to $R \times CN \times 2/n$CH, where R is the ratio of the Raman cross sections of water per OH divided by that of the solute per CH. The latter ratio was estimated from experimental measurements of CH areas of solutions of various alcohols of known concentration, divided by the OH area of pure water (scaled by the corresponding concentrations OH and CH groups in the two liquids). Concentration dependent measurements of the CH/OH areas of aqueous solutions indicate that the three solutes have R values of 1.22 for TBA, 1.32 for 2BA, and 1.27 for BE, and it is these values that were used to reconstruct hydration-shell spectra whose area matched the MD simulation prediction of the hydration-shell coordination numbers.

Conflicts of interest

There are no conflicts to declare.

Acknowledgements

This work was supported by a grant from the National Science Foundation (CHE-1763581). We thank Patrick Wise for help in performing the simulations used to obtain the hydration-shell coordination numbers.

References

1 P. Ball, Water as an active constituent in cell biology, *Chem. Rev.*, 2008, **108**, 74–108.
2 D. Laage, T. Elsaesser and J. T. Hynes, Water Dynamics in the Hydration Shells of Biomolecules, *Chem. Rev.*, 2017, **117**, 10694–10725.
3 E. Cabane, X. Y. Zhang, K. Langowska, C. G. Palivan and W. Meier, Stimuli-Responsive Polymers and Their Applications in Nanomedicine, *Biointerphases*, 2012, **7**, 9.
4 P. A. T. Martins, N. Domingues, C. Pires, A. M. Alves, T. Palmeira, J. Samelo, R. Cardoso, A. Velazquez-Campoy and M. J. Moreno, Molecular crowding effects on the distribution of amphiphiles in biological media, *Colloids Surf., B*, 2019, **180**, 319–325.
5 F. H. Stillinger, Structure in aqueous solutions of nonpolar solutes from the standpoint of scaled-particle theory, *J. Solution Chem.*, 1973, **2**, 141–158.
6 K. Lum, D. Chandler and J. D. Weeks, Hydrophobicity at Small and Large Length Scales, *J. Phys. Chem. B*, 1999, **103**, 4570–4577.
7 D. Chandler, Interfaces and the driving force of hydrophobic assembly, *Nature*, 2005, **437**, 640–647.
8 S. Rajamani, T. M. Truskett and S. Garde, Hydrophobic hydration from small to large lengthscales: Understanding and manipulating the crossover, *Proc. Natl. Acad. Sci. U. S. A.*, 2005, **102**, 9475–9480.
9 A. P. Willard and D. Chandler, The role of solvent fluctuations in hydrophobic assembly, *J. Phys. Chem. B*, 2008, **112**, 6187–6192.
10 E. Duboue-Dijon, A. C. Fogarty and D. Laage, Temperature Dependence of Hydrophobic Hydration Dynamics: From Retardation to Acceleration, *J. Phys. Chem. B*, 2014, **118**, 1574–1583.
11 V. R. Hande and S. Chakrabarty, Structural Order of Water Molecules around Hydrophobic Solutes: Length-Scale Dependence and Solute-Solvent Coupling, *J. Phys. Chem. B*, 2015, **119**, 11346–11357.
12 C. Petersen, K. J. Tielrooij and H. J. Bakker, Strong temperature dependence of water reorientation in hydrophobic hydration shells, *J. Chem. Phys.*, 2009, **130**, 214511.

13 I. T. S. Li and G. C. Walker, Signature of hydrophobic hydration in a single polymer, *Proc. Natl. Acad. Sci. U. S. A.*, 2011, **108**, 16527–16532.
14 I. T. S. Li and G. C. Walker, Single Polymer Studies of Hydrophobic Hydration, *Acc. Chem. Res.*, 2012, **45**, 2011–2021.
15 J. G. Davis, K. P. Gierszal, P. Wang and D. Ben-Amotz, Water structural transformation at molecular hydrophobic interfaces, *Nature*, 2012, **491**, 582–585.
16 X. E. Wu, W. J. Lu, L. M. Streacker, H. S. Ashbaugh and D. Ben-Amotz, Temperature-Dependent Hydrophobic Crossover Length Scale and Water Tetrahedral Order, *J. Phys. Chem. Lett.*, 2018, **9**, 1012–1017.
17 X. E. Wu, W. J. Lu, L. M. Streacker, H. S. Ashbaugh and D. Ben-Amotz, Methane Hydration-Shell Structure and Fragility, *Angew. Chem., Int. Ed.*, 2018, **57**, 15133–15137.
18 K. Mochizuki and D. Ben-Amotz, Hydration-Shell Transformation of Thermosensitive Aqueous Polymers, *J. Phys. Chem. Lett.*, 2017, **8**, 1360–1364.
19 F. Bohm, G. Schwaab and M. Havenith, Mapping Hydration Water around Alcohol Chains by THz Calorimetry, *Angew. Chem., Int. Ed.*, 2017, **56**, 9981–9985.
20 S. Lenton, N. H. Rhys, J. J. Towey, A. K. Soper and L. Dougan, Temperature-Dependent Segregation in Alcohol–Water Binary Mixtures is Driven by Water Clustering, *J. Phys. Chem. B*, 2018, **122**, 7884–7894.
21 A. K. Soper, L. Dougan, J. Crain and J. L. Finney, Excess entropy in alcohol–water solutions: A simple clustering explanation, *J. Phys. Chem. B*, 2006, **110**, 3472–3476.
22 S. Dixit, J. Crain, W. C. K. Poon, J. L. Finney and A. K. Soper, Molecular segregation observed in a concentrated alcohol–water solution, *Nature*, 2002, **416**, 829–832.
23 D. T. Bowron, A. K. Soper and J. L. Finney, Temperature dependence of the structure of a 0.06 mole fraction tertiary butanol-water solution, *J. Chem. Phys.*, 2001, **114**, 6203–6219.
24 D. Ben-Amotz, Hydration-Shell Vibrational Spectroscopy, *J. Am. Chem. Soc.*, 2019, **141**, 10569–10580.
25 A. Gao, L. Tan, M. I. Chaudhari, D. Asthagiri, L. R. Pratt, S. B. Rempe and J. D. Weeks, Role of Solute Attractive Forces in the Atomic-Scale Theory of Hydrophobic Effects, *J. Phys. Chem. B*, 2018, **122**, 6272–6276.
26 D. Ben-Amotz, Water-Mediated Hydrophobic Interactions, *Annu. Rev. Phys. Chem.*, 2016, **67**, 617–638.
27 D. S. Wilcox, B. M. Rankin and D. Ben-Amotz, Distinguishing Aggregation from Random Mixing in Aqueous *t*-Butyl Alcohol Solutions, *Faraday Discuss.*, 2013, **167**, 177–190.
28 B. M. Rankin, D. Ben-Amotz, S. T. van der Post and H. J. Bakker, Contacts Between Alcohols in Water Are Random Rather than Hydrophobic, *J. Phys. Chem. Lett.*, 2015, **6**, 688–692.
29 S. R. Pattenaude, B. M. Rankin, K. Mochizuki and D. Ben-Amotz, Water-mediated aggregation of 2-butoxyethanol, *Phys. Chem. Chem. Phys.*, 2016, **18**, 24937–24943.
30 N. Muller, Search for a Realistic View of the Hydrophobic Effect, *Acc. Chem. Res.*, 1990, **23**, 23–28.
31 P. N. Perera, K. R. Fega, C. Lawrence, E. J. Sundstrom, J. Tomlinson-Phillips and D. Ben-Amotz, Observation of water dangling OH bonds around dissolved nonpolar groups, *Proc. Natl. Acad. Sci. U. S. A.*, 2009, **106**, 12230–12234.
32 J. G. Davis, B. M. Rankin, K. P. Gierszal and D. Ben-Amotz, On the cooperative formation of non-hydrogen bonded water at molecular hydrophobic interfaces, *Nat. Chem.*, 2013, **5**, 796–802.
33 Q. Du, E. Freysz and Y. R. Shen, Surface Vibrational Spectroscopic Studies of Hydrogen-Bonding and Hydrophobicity, *Science*, 1994, **264**, 826–828.
34 J. Tomlinson-Phillips, J. Davis, D. Ben-Amotz, D. Spangberg, L. Pejov and K. Hermansson, Structure and Dynamics of Water Dangling OH Bonds in Hydrophobic Hydration Shells. Comparison of Simulation and Experiment, *J. Phys. Chem. A*, 2011, **115**, 6177–6183.
35 A. V. Plyasunov, N. V. Plyasunov and E. L. Shock, *The database for the thermodynamic properties of neutral compounds in the state of aqueous solution*, Department of Geological Sciences, Arizona State University, Tempe AZ 85287, 2005.
36 J. R. Errington and P. G. Debenedetti, Relationship between structural order and the anomalies of liquid water, *Nature*, 2001, **409**, 318–321.
37 E. D. Sloan, *Clathrate Hydrates of Natural Gases*, Marcel Dekker, New York, 1998.
38 K. Watanabe and H. C. Andersen, Molecular-Dynamics Study of the Hydrophobic Interaction in an Aqueous-Solution of Krypton, *J. Phys. Chem.*, 1986, **90**, 795–802.
39 P. R. TenWolde and D. Chandler, Drying-induced hydrophobic polymer collapse, *Proc. Natl. Acad. Sci. U. S. A.*, 2002, **99**, 6539–6543.
40 L. Tavagnacco, E. Zaccarelli and E. Chiessi, On the molecular origin of the cooperative coil-to-globule transition of poly(*N*-isopropylacrylamide) in water, *Phys. Chem. Chem. Phys.*, 2018, **20**, 9997–10010.
41 J. A. Long, B. M. Rankin and D. Ben-Amotz, Micelle Structure and Hydrophobic Hydration, *J. Am. Chem. Soc.*, 2015, **137**, 10809–10815.
42 S. M. Matt and D. Ben-Amotz, Influence of Intermolecular Coupling on the Vibrational Spectrum of Water, *J. Phys. Chem. B*, 2018, **122**, 5375–5380.
43 K. P. Gierszal, J. G. Davis, M. D. Hands, D. S. Wilcox, L. V. Slipchenko and D. Ben-Amotz, π-Hydrogen Bonding in Liquid Water, *J. Phys. Chem. Lett.*, 2011, **2**, 2930–2933.
44 P. Perera, M. Wyche, Y. Loethen and D. Ben-Amotz, Solute-Induced Perturbations of Solvent-Shell Molecules Observed Using Multivariate Raman Curve Resolution, *J. Am. Chem. Soc.*, 2008, **130**, 4576–4577.

